A PC-Interfaced, Compact Laser-Diode Feedback Interferometer for Displacement Measurements

Silvano Donati, *Member, IEEE*, Luca Falzoni, and Sabina Merlo

***Abstract*— We describe a laser-diode feedback interferometer for displacement measurements with directional discrimination and resolution better than 10^{-6} m. This new, compact instrument consists of a small optical head and a signal processing board, which is interfaced to a personal computer. The prototype developed has a dynamic range of 2 m and an accuracy of about 5 μm/m, using a corner cube as a remote reflector. Thanks to PC interfacing, the displacement is directly available in metric units and errors due to temperature fluctuations can be corrected with software signal processing.**

I. Introduction

LASER interferometry is a well-developed technique for displacement measurements with high resolution. Stabilized gas laser sources are usually employed when very high performance, such as resolution of 10^{-9} m and accuracy of 10^{-6} m, is desired. In these cases, the interferometric instrument is rather bulky and expensive. However, for many applications in industrial environment, resolution and accuracy of 10^{-6} m are sufficient but, on the other hand, very compact, lightweight, rugged and low-cost systems are required. For example, the accurate control of movements of machinery can be performed by displacement measurement along different axes, so that multiple measuring heads have to be applied and controlled. The possibility of easily interfacing the optical system to a personal computer becomes a very interesting feature.

In this paper, we present the prototype of a laser-diode feedback interferometer which can efficiently solve measuring problems in industrial processes. A very compact optical head is connected up to a PC-interfaced electronic board. Thanks to the selected interferometric configuration, the necessary optical components are limited to a collimating lens and a thin attenuator placed in the optical head and a corner cube as a backreflector. A commercial Fabry-Perot semiconductor laser emitting at $\lambda \approx 854$ nm has been selected. The emitted power propagating in open air is limited to 120 μW so that a well-developed instrument based on this principle would not imply safety problems in industrial environment.

II. Principle of Operation

A. Laser-Diode Feedback Interferometry

Laser feedback interferometry is an interesting alternative to the classical interferometric configurations. A small fraction of the emitted power is reflected back and reinjected inside the laser cavity by means of a remote reflective target. Amplitude and frequency modulation of the electric field are induced when a variation of the optical pathlength in the external cavity occurs: this perturbation of the laser field is indicated as feedback-induced modulation or self-mixing effect. If a semiconductor laser is used, the behavior of the system is described by the Lang and Kobayashi equations [1]. In a previous paper [2], we derived from these equations the expressions for the induced modulation effect on laser output power and frequency. We now recall the most important results and the meaning of the various parameters listed in Table I. The output power variation ΔP due to feedback with respect to the unperturbed laser can be written as

$$\Delta P = \Delta P_{\mathrm{MAX}} \cos \omega_F \tau \tag{1}$$

where ω_F is the laser oscillation frequency in case of feedback, which is related to the unperturbed oscillation frequency ω_0 by the following equation

$$\omega_0 \tau = \omega_F \tau + C \sin(\omega_F \tau + \arctan \alpha). \tag{2}$$

The feedback parameter C is given by

$$C = \frac{\varepsilon(1 - r_L^2) r_{\mathrm{ext}}}{r_L} \frac{\tau\sqrt{1+\alpha^2}}{\tau_L} \tag{3}$$

and is, thus, directly proportional to the fraction of the emitted electric field which is reinjected inside the cavity. It is well known that for a moving target

$$\omega_0 \tau = 2k[L + s(t)] \tag{4}$$

where $s(t)$ is the object displacement from a starting position L.

TABLE I
List of Parameters

α	linewidth enhancement factor (=6)
ω_{F}	effective oscillation frequency with feedback
ω_0	unperturbed laser oscillation frequency
τ	external cavity round trip time
τ_{L}	diode cavity round trip time (=8.3 ps)
$1/\tau_{\mathrm{L}}$	mode spacing (=120.41 GHz)
r_{L}	laser-facet field-reflectivity (=0.56)
r_{ext}	external mirror reflectivity
ε	coupling efficiency
k	$k = 2\pi/\lambda$
ϕ_0	$\phi_0 = 2kL$
λ	laser emission wavelength

Manuscript received August 12, 1995; revised June 18, 1996. This work was supported under a MURST 40% Contract.
The authors are with the Dipartimento di Elettronica, Università di Pavia, I-27100 Pavia, Italy.
Publisher Item Identifier S 0018-9456(96)08277-0.

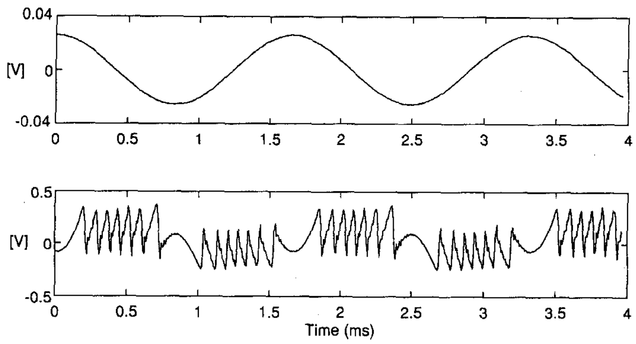

Fig. 1. Experimental signal typically detected in the moderate feedback regime. Upper trace: loudspeaker driving signal $s(t)$, corresponding to a peak-to-peak displacement of about 3 μm. Lower trace: detected signal after amplification with hysteresis and abrupt transitions.

For extremely weak feedback levels ($C \approx 0$) the output power is given by

$$\Delta P(t) = \Delta P_{\mathrm{MAX}} \cos[2ks(t) + \phi_0]. \tag{5}$$

Direct detection of the output power by means of a photodiode placed in front of the rear laser facet generates a current signal directly proportional to the interferometric signal $\cos[2ks(t)]$. Target displacement can be recovered but directional ambiguity cannot be solved. Frequently, in case of velocimetry, the object moving direction is known and the amplitude modulation effect can be used for velocity measurements, as it has been reported in [3]–[9]. For extremely weak feedback, as in the case of scattered light coupled back inside the laser cavity, the photodetected current is modulated at the Doppler frequency, $\omega_D = (4\pi/\lambda)v\cos\theta$ where v is the target velocity and θ is the angle between the direction of motion and the laser beam.

However, for larger fractions of output power coupled back inside the cavity, the approximation of (5) does not hold any longer. Experimentally it has been observed that the photo-generated current $I(t)$ becomes more and more distorted until it assumes a sawtooth-like behavior [2]. For moderate feedback levels ($1 < C < 4.6$) the function $\cos\omega_F\tau$ versus $\omega_0\tau$ exhibits bistability with hysteresis, and a wider hysteresis corresponds to a higher level of back reflection inside the cavity. In the presence of bistability, abrupt downward and upward transitions appear with periods $\omega_0\tau = 2\pi$ for increasing and decreasing optical phase delay. Therefore, transitions occur in the photo-generated current every time the target is displaced by $\Delta s = \lambda/2$. In Fig. 1, we show the typical detected signal in the moderate feedback regime when the reflector is mounted on a loudspeaker driven by a waveform generator.

If the detected signal is differentiated, positive and negative pulses are generated for upward and downward transitions, respectively. In a moderate feedback, the pulse counting configuration provides a resolution of $\lambda/2$ for object displacement, and the displacement direction is easily obtained from the polarity of the pulses counted with an up-down counter. This possibility has been proposed for the first time in [2] and has been exploited for the development of the instrument prototype described in this paper. Target velocity could also be recovered by measurement of pulse repetition rate, as reported in [10]–[11]. Incidentally, for $C > 4.6$ multistability occurs and, thus, the feedback interferometer should never work in this regime.

In case of a standing target, amplitude and frequency modulation are induced in the presence of back reflection if the laser emission wavelength is changed [(1)–(2)]. For example, if we modulate the laser-diode pumping current with a triangular waveform, both emission wavelength and output power are modulated. The induced modulation effect in the detected signal is superimposed on the triangular waveform of the output power and can be easily obtained by subtraction of the modulating wave. In our prototype, we have exploited this signal for remote reflector alignment, since reinjection inside the laser can be optimized by maximization of the hysteresis, as long as a suitable attenuator is placed in front of the laser in order to avoid multistability. Other authors have investigated this effect for ranging [12]–[13]. If the signal is differentiated, pulses occur with a repetition frequency which is proportional to the external cavity length.

B. Setup Configuration

The prototype is composed of an optical head connected to a signal processing board which is interfaced to a computer. A block diagram of the instrument is shown in Fig. 2(a). The head contains the laser source, a collimating lens, a variable attenuator, a thermoelectric cooler (TEC), a temperature sensor, and a preamplifier. All the components of the optical head [Fig. 2(b)] fit in a box of dimensions 20 mm × 20 mm × 50 mm (length).

The laser source is a Mitsubishi ML2701 AlGaAs Fabry-Perot laser-diode (single longitudinal mode), with a threshold current of 18 mA. The laser is pumped with a continuous current of 40 mA at which it emits an output power of 6.15 mW at a wavelength of about 853.2 nm. The monitor photodiode contained in the laser package is used for signal detection and the signal current (with the abrupt transitions) is superimposed on a continuous component ($I_M \approx 1$ mA).

The laser beam is collimated by an objective lens with antireflection coating at 850 nm, numerical aperture 0.45 and nominal focal length 4.5 mm; the lens mounting allows focusing the laser beam by varying the relative distance between the lens and the laser-diode. After being collimated the beam is attenuated to operate the source in the moderate feedback regime: the variable attenuator consists of a neutral density filter which has a power transmission $\approx$3% in the near infrared range, followed by a sheet (linear) polarizer; since polarized radiation is emitted from the laser-diode a fine adjustment of the attenuation level can be achieved by rotating the attenuator mounting. For proper operation of the interferometer the total power transmission must not exceed $\approx$2%, when using a corner cube as a backreflector, to avoid multistability.

The laser-diode temperature can be adjusted by means of the TEC, which is fed by an external current generator, so that the laser package temperature is maintained in a range in which no mode hopping occurs. An integrated sensor in thermal contact with the laser-diode holder detects the source temperature.

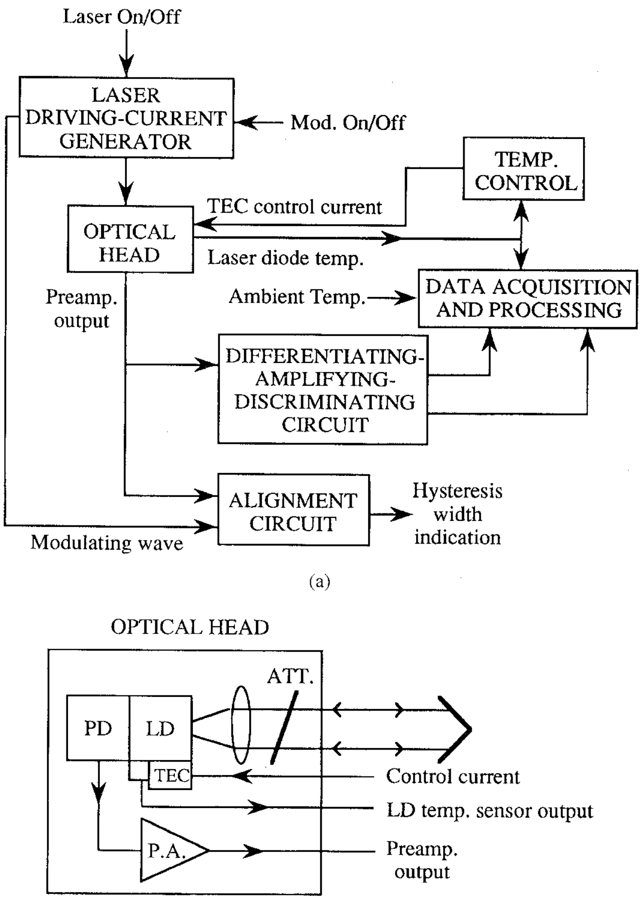

(b)

Fig. 2. (a) Block diagram of the instrument and (b) optical head scheme.

The photodiode signal current is preamplified by an ac-coupled transimpedance stage. The preamplifying circuit is shown in Fig. 3; the selected operational amplifier (MAX437CPA) has high gain-bandwidth product (60 MHz) and high open-loop gain (typ. $2 \cdot 10^7$). The photodiode is connected up to the negative power supply via a low-pass filter to eliminate interferences; the resistance R_1 keeps the photodiode reverse-biased with a 10 V voltage. The voltage drop across this resistance can be used as a control signal, providing a monitor of the laser power emission. Assuming the operational amplifier has an infinite gain, the transfer function is

$$\frac{V_{\text{out}}}{I_{\text{ph}}} = R_f \frac{sR_1C}{1+s(R_1+R_2)C} \tag{6}$$

which is a high-pass function with corner frequency $f_1 = \frac{1}{2\pi(R_1+R_2)C} = 76$ Hz, so that the dc component is filtered out and only the signal is amplified (the fast transitions at the preamplifier output have an amplitude of about 100 mV). The preamplifier feedback transfer function $\beta = \beta(s)$ is

$$\beta = \frac{1+s(R_1+R_2)C}{1+s(R_1+R_2+R_f)C}. \tag{7}$$

At the signal frequencies $f > f_1, \beta \approx 0.0645$; thus, the preamplifier total bandwidth is $60 \text{ MHz} \cdot 0.0645 = 3.87$ MHz.

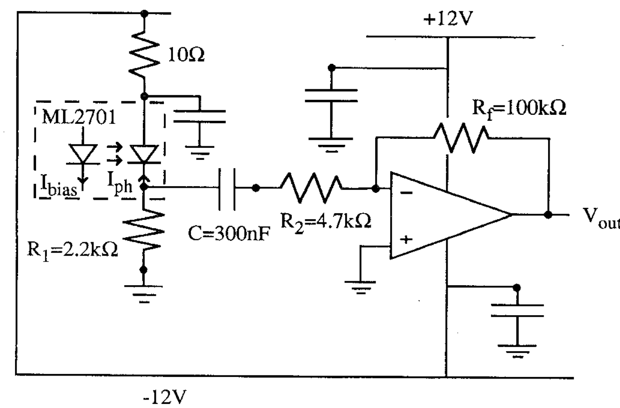

Fig. 3. AC-coupled preamplifying circuit.

The signal processing unit contains three circuit blocks:

—the differentiating-amplifying-discriminating circuit;
—the laser driving-current generator;
—the circuit for signal processing in the alignment phase.

The preamplifier output is fed to a high-pass filter (with $f_T \approx 48$ kHz) which differentiates the signal; the positive and negative pulses are amplified and separated on two different channels. Pulse shaping is achieved by means of two monostable multivibrators.

The laser current generator has been designed to protect the laser-diode as much as possible, since the instrument must be able to work properly in harsh environments. Its main characteristics are:

—slow-start of the pump current;
—protection against voltage and current spikes;
—protection against excessive direct current through the laser;
—protection against excessive reverse voltage across the junction;
—current stability within 1 μA.

A triangular wave with peak-to-peak amplitude of 1 mA and frequency of 3.4 kHz can be superimposed on the bias current so that the emission wavelength itself can be modulated (the laser has a specified coefficient $d\lambda/dI = 0.014$ nm/mA). This gives rise to a variation of the optical pathlength in the external cavity even when the reflector is not moving. The modulating triangular wave and the preamplifier output are sent to a subtractor; its output (that is, the induced modulation signal) is fed to a rms-value circuit that provides the user with an indication proportional to the hysteresis width. Automatic alignment could be performed by exploiting this principle.

The electronic unit is interfaced to the PC by means of a data-acquisition (DA) board. Connection between the electronic unit and the DA board has been realized with low input current, high-gain optocouplers, driven by the multivibrators. The use of optocouplers guarantees ground isolation between the two subsystems. Pulse counting is performed via software by continuously monitoring the logic state of the handshaking request lines of the DA board, which are connected up to the outputs of the optocouplers. Two variables for forward and backward displacement are incremented on the trailing edge of the respective handshaking signal and the overall target displacement (in counts with sign) is equal to the difference of the two variables. The total number of acquired counts is corrected to compensate for wavelength and, if necessary, air refractive index fluctuations due to temperature variations, as explained in details in Section IV. Laser and room temperature can be acquired by the PC through the DA board by means of a 12-bit ADC. Finally, the corrected number of counts is converted into metric displacement.

III. Performance

The theoretical linear relation between the number N_0 of counted pulses and the displacement L_0, as long as we are in the moderate feedback regime, is given by

$$L_0 = N_0 \frac{\lambda_0}{2n_0} \tag{8}$$

where $\lambda = \lambda_0$ is the laser emission wavelength at a well-determined value T_{0LD} of the laser package, $n = n_0$ is the air refractive index at a fixed value T_0 of room temperature, and $N_0 = N(n_0, L_0, \lambda_0)$ that is at well-defined and stable conditions. For verification of relationship (8), measurements have been performed for various displacements by moving the reflector back and forth between side-stops, placed at various distances from the optical head. Incidentally, we have observed that some problems arise because of the imperfect mechanical stability of the corner cube holder; this defect causes a repositioning error of about ± 3 μm. Measurement repeatability is also affected by thermal expansion of the optical table, which supports the interferometric setup, and of the mountings. Length variations are given by the relation

$$\frac{\Delta L}{L_0} = \alpha \Delta T \tag{9}$$

where α is the coefficient of thermal linear expansion (for example $\alpha = 22.32$ μm/m/°C for aluminum).

For laser-target distances less than 0.3 m, we have observed that hysteresis width becomes too low and instrument performance is limited in terms of mechanical noise immunity. For laser-target distances greater than 2.3 m the amplitude of the signal transitions shows fluctuations, so that reliable pulse counting will probably require a circuit for automatic gain control. With the present prototype we can thus ensure a linear response on a 2 m dynamic range at laser-target distances in the 0.3 to 2.3 m interval.

Another important feature of the instrument is maximum target velocity. Limitations on target speed arise only from electronic response time, while bistability is a consequence of optical feedback phenomena not affected by backreflector behavior. An upper limit is determined by the overall electronic bandwidth B, since $v_{\max} = \frac{\lambda}{2} \cdot \frac{1}{2t_r}$, where $t_r = \frac{0.35}{B} =$ signal rise time.

IV. Data Correction

In practice, the actual number of counts N is

$$N = N(n, L, \lambda) \tag{10}$$

where, $n = n_0 + \Delta n, L = L_0 + \Delta L, \lambda = \lambda_0 + \Delta\lambda$, since λ depends on laser temperature and bias current, n is a function of room temperature, atmospheric pressure and wavelength, and L is subject to thermal expansion. Therefore, all these parameters, as well as the number of counts N, are sensitive to ambient fluctuations.

Since $\Delta n, \Delta L, \Delta\lambda$ are small when compared to n_0, L_0, λ_0, (10) can be expressed as a Taylor series truncated at the first order

$$N = N(n_0, L_0, \lambda_0) + \frac{\partial N}{\partial n}\Delta n + \frac{\partial N}{\partial L}\Delta L + \frac{\partial N}{\partial \lambda}\Delta\lambda = N_0 + \Delta N. \tag{11}$$

Thus, the number N of counts, which is obtained during a measurement, is the sum of the expected value N_0 plus a corrective term ΔN due to fluctuations. Equation (8) should then be rewritten as

$$L_0 = (N - \Delta N)\frac{\lambda_0}{2n_0} = N\left(1 - \frac{\Delta N}{N}\right)\frac{\lambda_0}{2n_0}. \tag{12}$$

Since ΔN is small with respect to $N_0, \Delta N/N \approx \Delta N/N_0$ and (12) can be expressed in the form

$$L_0 = N\left(1 - \frac{\Delta N}{N_0}\right)\frac{\lambda_0}{2n_0}. \tag{13}$$

The error in the number of counts is

$$\begin{aligned}\frac{\Delta N}{N_0} &= \frac{\Delta n}{n_0} + \frac{\Delta L}{L_0} - \frac{\Delta\lambda}{\lambda_0}\\ &= \frac{1}{n_0}\left[\frac{\partial n}{\partial T}\Delta T + \frac{\partial n}{\partial P}\Delta P\right] + \frac{1}{L_0}\frac{dL}{dT}\Delta T\\ &\quad - \frac{1}{\lambda_0}\left[\frac{\partial\lambda}{\partial T_{\mathrm{LD}}}\Delta T_{\mathrm{LD}} + \frac{\partial\lambda}{\partial I_{\mathrm{BIAS}}}\Delta I_{\mathrm{BIAS}}\right].\end{aligned} \tag{14}$$

Now, a quantitative evaluation of the error contributions must be performed. The air refractive index can be calculated by means of a simplified version of the Edlén formula [14]

$$n = 1 + 10^{-6}\left(272.6 + \frac{4.608}{\lambda} + \frac{0.0606}{\lambda^2}\right)\frac{P}{760}\frac{288.15}{T} \tag{15}$$

in which λ is the emission wavelength in μm, P the atmospheric pressure in mmHg and T the air absolute temperature. Assuming $T = T_0 = 293.15$ K, $P = P_0 = 760$ mmHg and $\lambda = \lambda_0 = 853.2$ nm, it can be easily calculated that $(\partial n/\partial T)/n_0 = -0.93 \cdot 10^{-6}$/°C, $(\partial n/\partial P)/n_0 = 0.36 \cdot 10^{-6}$/mmHg. The coefficient $\partial n/\partial\lambda$ can be neglected, since its value is about $-6.3 \cdot 10^{-9}$/nm.

More importantly, we now consider the error contributions due to the intrinsic characteristic of the optical head and the coefficients $\partial\lambda/\partial T_{\mathrm{LD}}$ and $\partial\lambda/\partial I_{\mathrm{BIAS}}$ are evaluated. As previously mentioned, we have $\partial\lambda/\partial I_{\mathrm{BIAS}} = 0.014$ nm/mA, which implies that $-(1/\lambda_0)(\partial\lambda/\partial I_{\mathrm{BIAS}}) = -16.4$ pm/μm/mA; thus, emission wavelength fluctuations with bias current variations are negligible.

To evaluate the coefficient $\partial\lambda/\partial T_{\mathrm{LD}}$ a set of measurements has been performed in which the laser temperature has been varied by means of the TEC, and pulse counting has been recorded with a standing backreflector to avoid the repositioning error of the corner cube. Every single measurement has been performed by cooling the laser diode with a $\Delta T_{\mathrm{LD}} = -2.28$°C (maximum possible thermal excursion for a linear

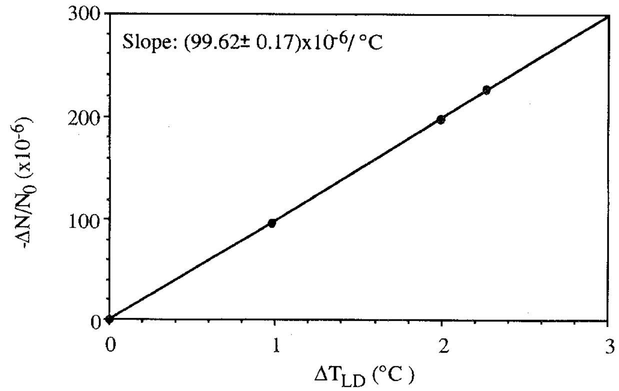

Fig. 4. Corrective term for the number of counts, in case of laser temperature variations. Adjusted standard deviation is equal to 1.365 $10^{-6}/°C$ and is within the size of the dots.

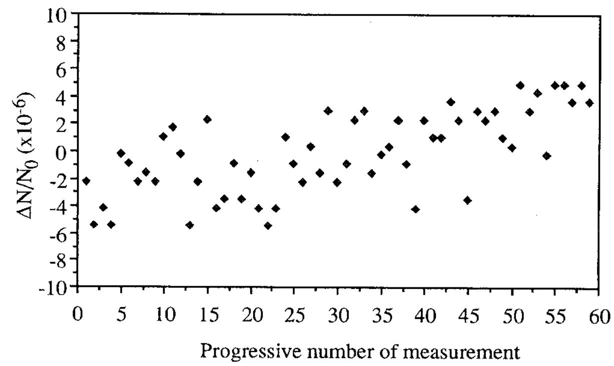

Fig. 5. Experimental residual error obtained with standing target after compensation of laser temperature variations. Every data point corresponds to a 2.28 °C temperature sweep of the laser.

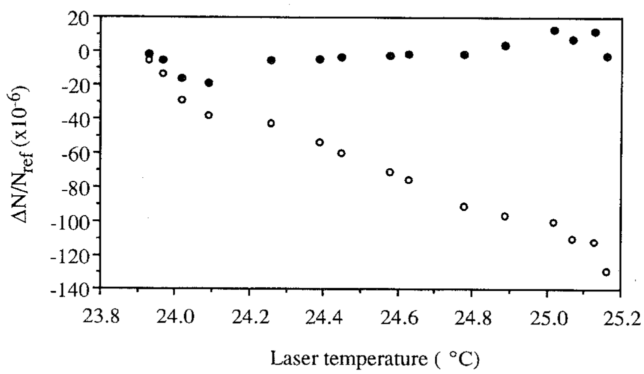

Fig. 6. $\Delta N/N_{\rm ref}$ versus laser temperature, obtained for 22-cm target displacements: o experimental data before compensation, • compensated results.

variation of λ with $T_{\rm LD}$), which is much greater than room temperature fluctuations; under such conditions, the error is almost entirely due to the laser wavelength sweep

$$\frac{\Delta N}{N_0} = -\frac{\Delta\lambda}{\lambda_0} = -\frac{\alpha_\lambda \Delta T_{\rm LD}}{\lambda_0} \tag{16}$$

where $\alpha_\lambda = \frac{\partial\lambda}{\partial T_{\rm LD}}$.

The measurements have been repeated several times in order to carry out a statistical analysis [15] and after $m = 65$ measurements the following results have been obtained:

—the best estimate $\langle\alpha_\lambda\rangle$ of the true value of α_λ

$$\langle\alpha_\lambda\rangle = -\frac{\lambda_0}{N_0}\frac{\langle\Delta N\rangle}{\Delta T_{\rm LD}} = \lambda_0 \cdot 99.62 \cdot 10^{-6}/°{\rm C}^{-1} \tag{17}$$

where $N_0 = 2L_0/\lambda_0$, with laser-target distance $L_0 = 658$ mm;

—the best estimate of the standard deviation of α_λ (adjusted standard deviation)

$$\begin{aligned} s_m(\alpha_\lambda) &= \langle\alpha_\lambda\rangle \frac{\sigma(\Delta N)}{\langle\Delta N\rangle}\sqrt{\frac{m}{m-1}} \\ &= \lambda_0 \cdot 1.365 \cdot 10^{-6}/°{\rm C}^{-1} \end{aligned} \tag{18}$$

—the best estimate of the standard error of α_λ (adjusted standard error)

$$S_m(\alpha_\lambda) = \frac{s_m(\alpha_\lambda)}{\sqrt{m}} = \lambda_0 \cdot 0.17 \cdot 10^{-6}/°{\rm C}^{-1}. \tag{19}$$

Therefore, the true value of α_λ is given by

$$\alpha_\lambda = \lambda_0 \cdot (99.62 \pm 0.17) \cdot 10^{-6}/°{\rm C}^{-1} \tag{20}$$

as reported in Fig. 4.

We have used (20) to compensate wavelength fluctuations in a new set of data collected as in the previous measurement with the standing reflector and in Fig. 5 we present the residual error after compensation. Notice that for a laser temperature change $\Delta T_{\rm LD} = 2$ °C, the error $\Delta N/N_0$ would be of the order of $2 \cdot 10^{-4}$; after compensation such an error is reduced within $\pm 5 \cdot 10^{-6}$ which could be due to fluctuations of ambient parameters.

As already mentioned in Section III, the instrument has been tested with repeated displacement measurements to simulate real working conditions; among all the experimental data we have chosen a set of measurements relative to a 22-cm displacement. In this set, laser temperature has been gradually increased before every single measurement so that $T_{\rm LD}$ was constant during the displacement. The number of counts has been collected every time and variations ΔN have been calculated with respect to the first count ($N_{\rm ref}$). In Fig. 6 the variation $\Delta N/N_{\rm ref}$ is shown as a function of laser temperature before and after compensation. The residual error is maintained within $\pm 20 \cdot 10^{-6}$, which takes into account the repositioning error previously evaluated (the error of ± 3 μm corresponds to $\pm 15 \cdot 10^{-6}$ on a 22-cm displacement).

Since we have demonstrated the validity of the compensation method we can state that the overall displacement L_0 relative to a number N of counts can thus be obtained by the following relationship (to be implemented on the PC)

$$\begin{aligned} L_0 = N\{1 + 10^{-6} \cdot [&0.93 \cdot (T - T_0) \\ &+ 99.62 \cdot (T_{\rm LD} - T_{\rm 0LD})]\}\frac{\lambda_0}{2n_0} \end{aligned} \tag{21}$$

where thermal expansion has been neglected.

V. Conclusion

We have demonstrated that laser-diode feedback interferometry allows us to overcome limitations set by spectral characteristics of Fabry–Perot semiconductor lasers and to perform displacement measurements with high resolution and directional discrimination on a sufficiently wide dynamic range.

Nevertheless, wavelength stability of $\Delta\lambda/\lambda \approx 10^{-6}$ is usually required in interferometric measurements. Such a stability could be obtained for example with a temperature stabilization of the laser source within 0.01 °C, which would require a sophisticated control system, thus increasing instrument complexity and cost.

Alternatively, we have verified that a comparable accuracy is achievable with a temperature stabilization limited to ± 1 °C (to avoid laser mode hopping) followed by a compensation of small variations of the laser wavelength, and eventually of the air refractive index. Thanks to PC interfacing this error correction can be easily performed.

In conclusion, we have demonstrated a novel interferometric instrument for displacement measurement, which consists of a very compact optical head and a signal processing unit: prototype accuracy is comparable to that of classical configurations, which are usually much larger and expensive.

References

[1] R. Lang and K. Kobayashi, "External optical feedback effects on semiconductor injection laser properties," *IEEE J. Quantum Electron.*, vol. QE-16, no. 3, pp. 347–355, 1980.

[2] S. Donati, G. Giuliani, and S. Merlo, "Laser diode feedback interferometer for measurements of displacement without ambiguity," *IEEE J. Quantum Electron.*, vol. 31, no. 1, pp. 113–119, 1995.

[3] S. Shinoara, A. Mochizuki, H. Yoshida, and M. Sumi, "Laser Doppler velocimeter using the self-mixing effect of a semiconductor laser diode," *Appl. Opt.*, vol. 25, no. 9, pp. 1417–1419, 1986.

[4] P. J. de Groot, G. M. Gallatin, and S. H. Macomber, "Ranging and velocimetry signal generation in a backscatter-modulated laser diode," *Appl. Opt.*, vol. 27, no. 21, pp. 4475–4480, 1988.

[5] H. W. Jentink, F. F. M. de Mul, H. E. Suichies, J. G. Aarnoudse, and J. Greve, "Small laser Doppler velocimeter based on the self-mixing effect in a diode laser," *Appl. Opt.*, vol. 27, no. 2, pp. 379–385, 1988.

[6] F. F. M. de Mul, M. H. Koelink, A. L. Weijers, J. Greve, J. G. Aarnoudse, R. Graaff, and A. C. M. Dassel, "Self-mixing laser-Doppler velocimetry of liquid flow and of blood perfusion in tissue," *Appl. Opt.*, vol. 31, no. 27, pp. 5844–5851, 1992.

[7] ——, "A semiconductor laser used for direct measurement of the blood perfusion of tissue," *IEEE Trans. Biomed. Eng.*, vol. 40, no. 1, pp. 208–210, 1993.

[8] K. Mito, H. Ikeda, M. Sumi, and S. Shinoara, "Self-mixing effect of the semiconductor laser Doppler method for blood flow measurement," *Med. Biol. Eng. Comput.*, vol. 31, pp. 308–310, 1993.

[9] M. H. Koelink, M. Slot, F. F. M. de Mul, J. Greve, R. Graaff, A. C. M. Dassel, and J. G. Aarnoudse, "Laser-Doppler velocimeter based on the self-mixing effect in a fiber-coupled semiconductor laser: Theory," *Appl. Opt.*, vol. 31, no. 18, pp. 3401–3408, 1992.

[10] E. T. Shimizu, "Directional discrimination in the self-mixing type laser Doppler velocimeter," *Appl. Opt.*, vol. 26, no. 21, pp. 4541–4544, 1987.

[11] S. Shinoara, H. Naito, H. Yoshida, H. Ikeda, and M. Sumi, "Compact and versatile self-mixing type laser Doppler velocimeter with direction-discrimination circuit," *IEEE Trans. Instrum. Meas.*, vol. 38, no. 2, pp. 574–577, 1989.

[12] G. Beheim, and K. Fritsch, "Range finding using frequency modulated laser diode," *Appl. Opt.*, vol. 25, no. 9, pp. 1439–1442, 1986.

[13] S. Shinoara, H. Yoshida, H. Ikeda, K.-I. Nishide, and M. Sumi, "Compact and high-precision range finder with wide dynamic range and its application," *IEEE Trans. Instrum. Meas.*, vol. 41, no. 1, pp. 40–44, 1992.

[14] B. Edlén, "The refractive index of air," *Metrologia*, vol. 2, pp. 71–80, 1966.

[15] N. C. Barford, *Experimental Measurements: Precision, Error and Truth.* New York: Wiley, 1985, ch. 2.

Silvano Donati (M'75) received the degree in physics (*cum laude*) from the University of Milano, Milano, Italy, in 1966.

From 1966 to 1975 he was with CISE, Milano, working on noise in photomultipliers and avalanche photodiodes, nuclear electronics, and electrooptic instrumentation (laser telemetry, speckle pattern interferometry, and gated vision in scattering media). In 1975, he joined the Department of Electronics, University of Pavia, Pavia, Italy, as Internal Lecturer of Electronics Laboratory, and worked on interferometers, fiber gyroscope and noise in CCD's. In 1980, he became Full Professor of Electrooptical Systems, and since then, his main research interests have been with optical fiber sensors, passive fiber components for telecommunications, free-space, and guided optical interconnections. He promoted several programs of R&D cooperation with national companies, active in the areas of optical communications, laser instrumentation and avionics. He has authored or coauthored over 130 papers and holds four patents.

Dr. Donati is a member of AEI, APS/OSA, and ISHM, and has actively served to organize several national and international meetings and schools in the steering and program committees or as a chairman. He also works in the standardization activity of CEI/IEC (CT-76 laser safety and CT-86 optical fibers).

Luca Falzoni was born in Cilavegna, Italy, in 1970. He received the degree in electronic engineering in March, 1995, from the University of Pavia, Pavia, Italy.

Since then, he has been with the Electrooptics Laboratory, University of Pavia, working on the development of the induced modulation inteferometer prototype.

Sabina Merlo was born in Pavia, Italy, in 1962 and received the degree (*cum laude*) in electronic engineering from the University of Pavia in 1987, the M.S.E. degree in bioengineering from the University of Washington, Seattle, in 1989, and the Ph.D. degree in electronic engineering from the University of Pavia in 1991.

In 1993, she became a staff researcher, Department of Electronics, University of Pavia. Her main research interests include optical fiber sensors for the measurement of chemical and electrical parameters, advanced methods of photodetection, optical amplifiers, and laser interferometry. She holds three patents and is coauthor of about thirty papers.

Dr. Merlo was recipient of a Rotary Foundation Graduate Scholarship for studying at the University of Washington.